Brain-inspired recurrent neural network with plastic RRAM synapses

Valerio Milo
Dipartimento di Elettronica, Informazione e Bioingegneria
Politecnico di Milano and IU.NET
Milano, Italy 20133
email: valerio.milo@polimi.it

Elisabetta Chicca
Faculty of Technology and Cognitive Interaction Technology Center of Excellence (CITEC)
Bielefeld University, Bielefeld, Germany
email: chicca@cit-ec.uni-bielefeld.de

Daniele Ielmini
Dipartimento di Elettronica, Informazione e Bioingegneria
Politecnico di Milano and IU.NET
Milano, Italy 20133
email: daniele.ielmini@polimi.it

***Abstract*—The development of neuromorphic systems capable of mimicking the behavior of the human brain has recently received an increasing deal of interest. However, the building of such artificial systems has been hindered by the lack of commercial technologies with nanoscale integration of synaptic devices as well as the complexity of the biological neural architecture in terms of connectivity, parallelism, and plasticity behavior. In particular, there is a wide consensus on the relevance of recurrent connections in the human brain, and their key role for associative learning and pattern classification. Fundamental primitives of cognitive computing can therefore be demonstrated by means of Recurrent Neural Networks (RNNs).**

In this work, we design and simulate a Hopfield-type RNN with HfO_2 RRAM devices capable of learning via spike-timing dependent plasticity (STDP). We first demonstrate learning and recall of a single attractor state in a 4-neuron RNN. Based on this result, we then simulate signal restoration of two orthogonal patterns in a 64-neuron RNN, thus supporting RRAM-based RNN with cognitive computing functionalities.

Keywords: Neuromorphic computing; resistive switching memory (RRAM); spike-timing dependent plasticity (STDP); Hopfield network; associative memory.

I. Introduction

Neuromorphic computing systems are raising interest as non-von Neumann solutions for energy-efficient, highly parallel and error-tolerant data processing [1]. Although highly promising for cognitive tasks, such as image classification and speech recognition [2], [3], the grand challenge of realizing neuromorphic chips capable of emulating the human brain remains very far ahead. One of the big challenges in neuromorphic engineering is the achievement of synaptic density comparable to the biological one (about 10^4 synapses per neuron). Novel emerging technologies such as resistive-switching memory (RRAM) and phase-change memory (PCM) have been proposed as a mean for achieving such synaptic density. Specifically, nano-electronic synapses capable of brain-plausible learning rules such as spike-timing dependent plasticity (STDP) [4]–[12] and spike-rate dependent plasticity (SRDP) [9] have been used in the context of feed-forward neural networks. Another challenge is the identification and replication of key neural architectures supporting biological computational primitives. Recurrent synaptic connections are believed to be the origin of fundamental cognitive primitive functions, such as associative memory, sequence learning and context-dependent decision making [1], [13], [14]. This inspired the well established theoretical framework based on attractor neural networks [15] and the related technology developments based on either CMOS technology [16]–[19] or emerging memory devices such as RRAM [20]–[22] and PCM [14], [23].

In this work, we describe a simulated RNN architecture comprising plastic RRAM synapses with one-transistor/one-resistor (1T1R) structure. After demonstrating attractor learning and recall in a 4-neuron RNN, we simulate a larger RRAM-based RNN with 64 neurons to demonstrate pattern classification and restoration with two orthogonal stored attractors. Our results support the choice of RRAM-based RNNs as computational primitives for learning.

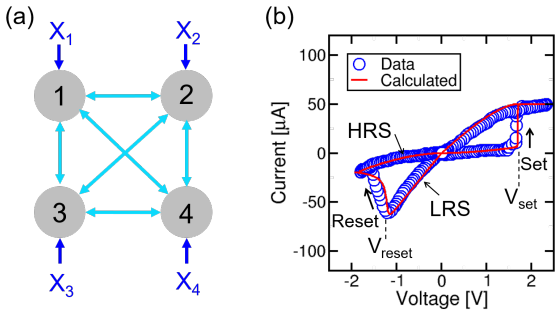

Fig. 1. (a) Illustrative representation of a 4-neuron Hopfield neural network with all-to-all connections. (b) Measured and calculated $I-V$ characteristics of the 1T1R synapse evidencing low resistance state (LRS) and high resistance state (HRS) which are achieved by set and reset transitions, respectively.

II. Hopfield RNN architecture

Hopfield-type RNN is a well-known network topology capable of performing associative learning which is a fundamental function in the mammalian brain [24]. Fig. 1(a) shows the

This work was supported in part by the European Research Council (grant ERC-2014-CoG-648635-RESCUE) and by the Cluster of Excellence Cognitive Interaction Technology 'CITEC' (EXC 277) at Bielefeld University, which is funded by the German Research Foundation (DFG).

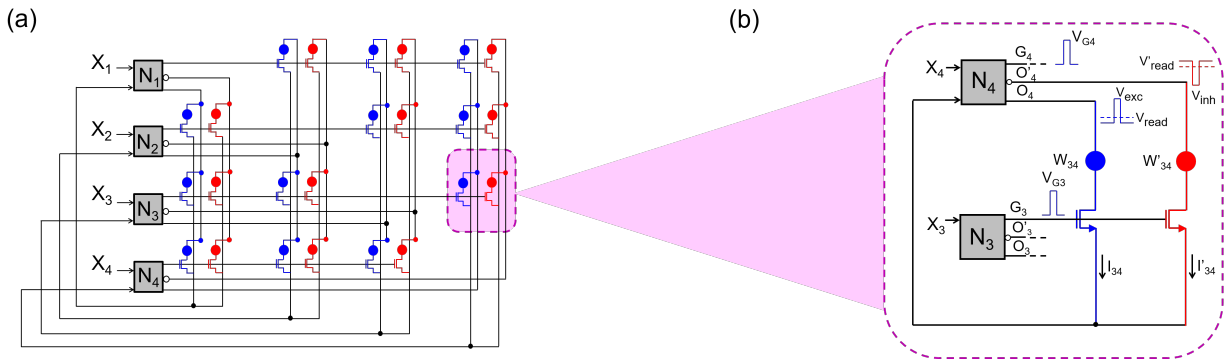

Fig. 2. (a) Circuital scheme of simulated 4-neuron Hopfield network with all-to-all excitatory (blue) and inhibitory (red) 1T1R synaptic connections. The lack of connections along the diagonal of the synaptic matrix indicates the absence of self-feedback. (b) Illustrative description of the network operation during training: the output pulse V_{G3} fired by neuron N_3 activates the excitatory and inhibitory connections of its synaptic row and in particular W_{34} and W'_{34} inducing the currents I_{34} and I'_{34}. If N_4 is coactive with N_3, the overlap between spikes causes LTP for W_{34} and LTD for W'_{34}.

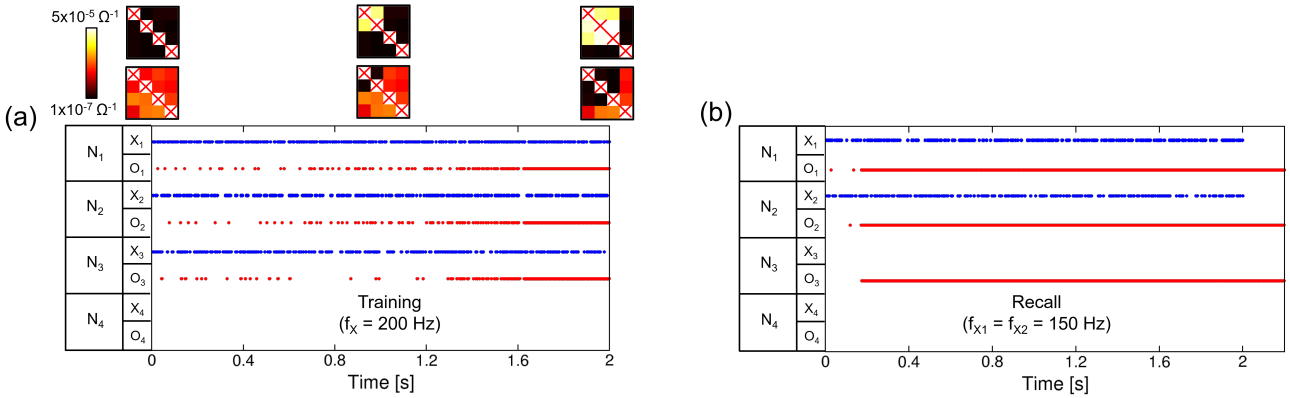

Fig. 3. (a) Attractor learning of a 4-neuron Hopfield RNN. (top) Starting from excitatory/inhibitory synapses in HRS/LRS, weight maps at times t = 0 s, t = 1 s and t = 2 s evidence learning of the network state defined by spiking activity of N_1-N_3 via gradual LTP/LTD of corresponding excitatory/inhibitory synapses. (bottom) The raster plot shows the external stimulation at f_X = 200 Hz (blue dots) and the spiking activity (red dots) of neurons during training. As a result of LTP/LTD of excitatory/inhibitory synapses, the firing activity of all stimulated neurons gradually increases until it becomes stable, hence supporting attractor formation. (b) Neuronal dynamics during recall process of the 4-neuron Hopfield network. The raster plot indicates that the external stimulation of a subset of N_1-N_3 pool enables to reactivate the full attractor state and to reach a sustained spiking activity even if the external spikes are removed.

conceptual scheme of a Hopfield spiking RNN consisting of 4 neurons receiving external stimuli X_i (i=1-4) as well as mutual spiking interactions via symmetric synapses. To explore RNN learning capabilities, we developed a model for a RNN equipped with 1T1R RRAM synapses capable of STDP [22]. Fig. 1(b) shows the measured and calculated $I-V$ characteristics of a 1T1R RRAM device used in this work [12]. Set and reset processes occur at voltages V_{set} and V_{reset}, thus enabling plastic long-term potentiation (LTP) and long-term depression (LTD) of the synaptic connection [9]. The switching behavior of simulated RRAM devices is captured by a variability-aware analytical model [25] capable of replicating the LRS and HRS distributions [22]. Fig. 2(a) shows the circuit implementation of the RNN with 4 leaky integrate and fire (LIF) neurons, fully connected via 12 excitatory (blue) and 12 inhibitory (red) plastic synapses. Each neuron in the RNN acts both as pre-synaptic neuron by driving the gates of 3 excitatory/inhibitory synapses along a row, and as post-synaptic neuron by driving the top electrodes (TEs) of 3 excitatory/inhibitory synapses along a column. Each neuron also receives external asynchronous current spikes and internal current spikes from the RNN. As the integrated current reaches a given threshold within a neuron N_i, the neuron fires, thus sending a positive voltage spike V_{Gi} to the gate of synapses in the *i*-th row and a positive (negative) voltage spike V_{exc} (V_{inh}) from output O_i (O'_i) to the TE of excitatory (inhibitory) synapses in the *i*-th column.

The synaptic dynamics in the network is further described in Fig. 2(b), showing the pair of N_3 as pre-synaptic neuron and N_4 as post-synaptic neuron, connected by an excitatory synapse of weight W_{34} and an inhibitory synapse of weight W'_{34}. As N_3 fires, V_{G3} activates the synapse gates by inducing the weighted synaptic currents I_{34} and I'_{34}. If N_4 fires at the same time as N_3, the time overlap of voltage spikes V_{G3} and $V_{exc} > V_{set}$ induces a conductance increase, hence causing LTP of W_{34}. On the other hand, the overlap of voltage spikes V_{G3} and $V_{inh} < V_{reset}$ induces a conductance decrease, hence causing LTD of W'_{34} [22]. Time-dependent

978-1-5386-4881-0/18/$31.00 ©2018 IEEE

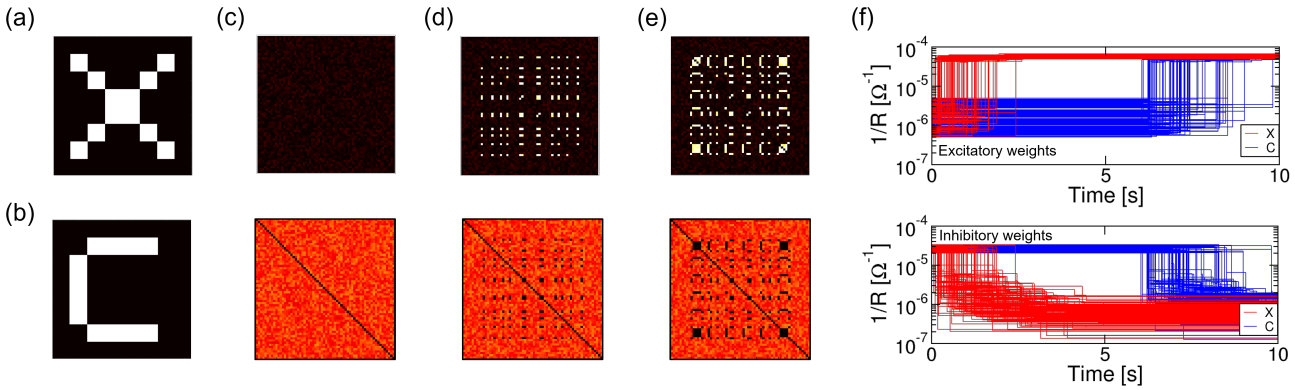

Fig. 4. (a) 'X' and (b) 'C' 8x8 input patterns used to train the simulated 64-neuron Hopfield network. Weight maps showing excitatory (top) and inhibitory (bottom) weights during training at times (c) t = 0 s, (d) t = 5 s, and (e) t = 10 s. (f) Time evolution of excitatory (top) and inhibitory (bottom) synapses during sequential storing of two attractors evidencing 'X' learning (t = 0-5 s) followed by 'C' learning (t = 5-10 s).

LTP and LTD realize Hebbian learning, where only synapses between coactive neurons undergo weight update, according to the STDP protocol. To this purpose, note that inhibitory synapses are essential during the learning process since they prevent neurons receiving no external spikes to fire, thus avoiding unwanted weight updates. After training, the network is operated in a *recall* mode by preventing the output spikes O_i and O'_i, which thus remain at read voltages V_{read} and V'_{read} = - V_{read}, respectively, not to induce any weight update.

III. Attractor Learning and Recall

Associative memory is a fundamental computational property of biological systems resulting from collective activity of a large population of neurons [24]. Associative memory enables to retrieve a previously stored neuronal activity state, called attractor, by stimulating only a part of the memory [14], [19], [20], [22]–[24]. For instance, Fig. 3(a) shows a 4-neuron RNN during training with neurons N_1, N_2, N_3 being active. All the excitatory synaptic weights are initially prepared in high resistance state (HRS) while the inhibitory weights in low resistance state (LRS). Note that the initial weight scheme plays an important role for RNN operation since it ensures the depression of the excitatory weights (as well as the potentiation of inhibitory weights) out of the attractor from the beginning of the learning process. Upon stimulation of the N_1-N_3 pool by external Poisson spike trains at average frequency f_X = 200 Hz, output spikes O_1-O_3 are increasingly generated as a result of synaptic plasticity, thus evidencing the formation of an attractor. This dynamics demonstrates Hebbian learning of an attractor with selective LTP (LTD) of excitatory (inhibitory) synapses among coactive neurons of the pool, while all other weights remain at their initial value.

After training, we tested the capability of the simulated RNN to recall the stored attractor state. Fig. 3(b) shows the recall dynamics for the 4-neuron RNN as only 2 attractor neurons receive external spikes. As a result of external stimulation (f_X = 150 Hz), the output spikes O_1 and O_2 induce N_3 reactivation leading to a sustained spiking activity of all the attractor neurons even as the external spikes are removed after t = 2 s.

IV. Pattern Completion by 8x8 Hopfield Network

A. Information storage

A key advantage of Hopfield RNNs is signal restoration. Several activation patterns can be stored within a RNN, and later recalled by the presentation of a noisy version of the learned pattern. To explore signal restoration capability, we simulated learning and recall of two 8x8 visual patterns within a 64-neuron RNN. First, the network was trained by sequentially submitting 2 patterns, starting with pattern 'X' (Fig. 4(a)) for 5 s, followed by pattern 'C' (Fig. 4(b)) for other 5 s. Note that the 2 patterns are non-overlapping, or orthogonal. Fig. 4(c-e) shows the excitatory (top) and inhibitory (bottom) weight maps during sequential training. Starting from excitatory/inhibitory weights in HRS/LRS (c), 'X' submission during the time interval 0-5 s leads to the formation of the first attractor (d). At t = 5 s, 'X' is replaced by 'C' as training pattern and its presentation for the following 5 s causes the storage of the second attractor, leading to the final weight configurations shown in Fig. 4(e). This sequential learning process is also supported by time evolution of excitatory (top) and inhibitory (bottom) weights in Fig. 4(f) indicating LTP of 'X' and 'C' excitatory synapses within 5 s and 10 s, respectively, and LTD of corresponding inhibitory synapses.

B. Signal restoration

The capability of signal restoration was studied by testing the 64-neuron RNN upon submission of a fraction of the original patterns 'X' and 'C' [14]. To this end, we submitted pattern 'X' but removed the input to some of the neurons, *e.g.*, only 9 (Fig. 5(a)) or 5 (Fig. 5(b)) active neurons out of 12, and observed the RNN response. Fig. 5(c) shows the increase with time of the number of spiking neurons within 'X' attractor in both cases. In case of 9 active neurons, the submitted partial pattern induces the activation of the total attractor within only 0.1 s. On the contrary, as the submitted information

978-1-5386-4881-0/18/$31.00 ©2018 IEEE

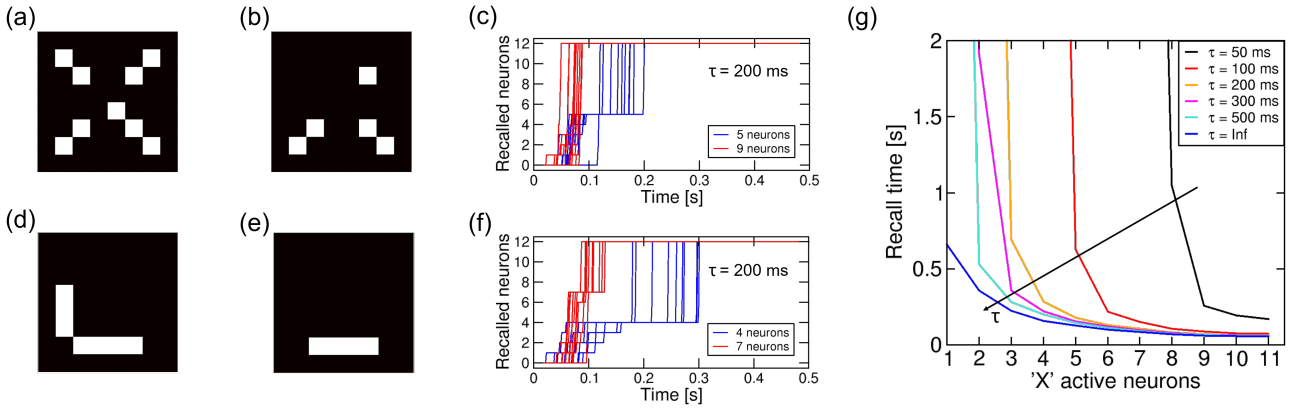

Fig. 5. Features of original pattern 'X' with (a) 9 and (b) 5 active input channels inducing the reactivation of all the 12 attractor neurons within about 0.1 s and 0.2 s, respectively (c). Incomplete versions of the original pattern 'C' with (d) 7 and (e) 4 active input channels leading to the reactivation of all the 12 attractor neurons within about 0.15 s and 0.3 s, respectively (f). (g) Average recall time of attractor 'X' as a function of density of submitted partial pattern for variable τ values.

becomes less accurate as in Fig. 5(b), the average time for the RNN to reactivate the attractor increases, *i.e.*, about 0.2 s. The same recall test was also conducted for the attractor 'C' assuming to test the network with two incomplete patterns with 7 (Fig. 5(d)) and 4 (Fig. 5(e)) active neurons, respectively. As expected, the retrieval of attractor 'C' is achieved for both input patterns (Fig. 5(f)), where the reactivation time increases for decreasing stimulated neurons.

Fig. 5(g) shows the calculated average recall time to retrieve 'X' as a function of the number of attractor neurons stimulated by external spikes. In the simulations, we assumed various values of τ, corresponding to various leakage during integration of incoming spikes. The recall time was defined as the time the network takes to reactivate all neurons of a stored memory. As τ increases, the recall time for a given number of initially active neurons decreases because leakage impact on the firing activity of recalled attractor neurons gradually decreases. Similarly, the minimum number of active neurons to restore the full pattern increases for decreasing τ as the discharge of internal potential within each neuron becomes gradually faster by preventing attractor neurons to fire. Note that the same result would be also obtained for 'C' since their density is equivalent.

C. Error correction

To test the error correction capability, we simulated the recall process of the 64-neuron RNN after training as in Fig. 5, upon submission of an erroneous pattern, *i.e.*, a pattern with features of both 'X' and 'C'. Fig. 6 shows a color plot summarizing all the results of 1000 simulation runs for each recall test. The plot shows the complementary probability of activating 'X' or 'C' attractor, where P = 0 and 1 correspond to pattern 'C' and 'X', respectively. As the submitted pattern becomes more similar to a pattern, the probability to recall that particular pattern increases. This is because the attractor with higher density is fed with a larger number of spikes, thus its activation spreads within the attractor strongly with time.

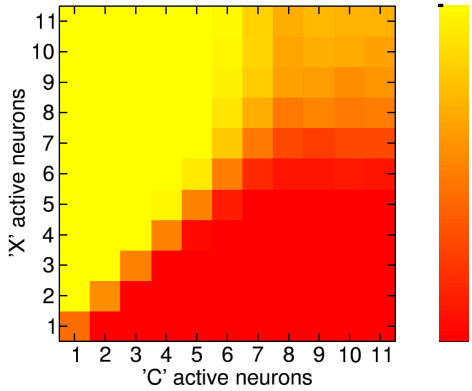

Fig. 6. Color map of recall probability P as features of both patterns with variable density test the 64-neuron Hopfield network at the same time.

On the other hand, if the submitted pattern contains equal shares of 'X' and 'C', P is approximately 0.5, *i.e.*, equal probabilities of recalling either pattern. Finally, as the density of 'X' and 'C' features in the input pattern is higher than 6 stimulated neurons, the recall probability assumes intermediate values since the capability of recalling one rather than the other attractor becomes more dependent on the stochastic nature of external stimulation (provided by the Poisson statistics of the input spike trains) than on the density of features.

V. Conclusions

In this paper, we have demonstrated the associative memory capabilities of a simulated Hopfield RNN based on 1T1R excitatory and inhibitory RRAM-based synapses capable of STDP. Furthermore, we have investigated pattern completion properties and temporal dynamics of attractor recall.

These results set the basis for future implementation of hybrid CMOS/RRAM-based neural networks for building brain-inspired computing systems.

978-1-5386-4881-0/18/$31.00 ©2018 IEEE

REFERENCES

[1] G. Indiveri and S.-C. Liu, "Memory and information processing in neuromorphic systems," *Proc. IEEE*, vol. 103, no. 8, pp. 1379–1397, 2015.

[2] Y. LeCun, Y. Bengio, and G. Hinton, "Deep learning," *Nature*, vol. 521, pp. 436–444, 2015.

[3] G. Hinton, L. Deng, D. Yu, G. E. Dahl, A. Mohamed, N. Jaitly, A. Senior, V. Vanhoucke, P. Nguyen, T. N. Sainath, and B. Kingsbury, "Deep neural networks for acoustic modeling in speech recognition," *IEEE Signal Processing Magazine*, vol. 29, no. 6, pp. 82–97, 2012.

[4] S. H. Jo, T. Chang, I. Ebong, B. B. Bhadviya, P. Mazumder, and W. Lu, "Nanoscale memristor device as synapse in neuromorphic systems," *Nano Lett.*, vol. 10, no. 4, pp. 1297–1301, 2010.

[5] M. Suri, O. Bichler, D. Querlioz, O. Cueto, L. Perniola, V. Sousa, D. Vuillaume, C. Gamrat, and B. DeSalvo, "Phase change memory as synapse for ultra-dense neuromorphic systems: application to complex visual pattern extraction," *IEDM Tech. Dig.*, pp. 79–82, 2011.

[6] S. Yu, B. Gao, Z. Fang, H. Yu, J. Kang, and H.-S. P. Wong, "A neuromorphic visual system using RRAM synaptic devices with sub-pJ energy and tolerance to variability: experimental characterization and large scale modeling," *IEDM Tech. Dig.*, pp. 239–242, 2012.

[7] S. Ambrogio, N. Ciocchini, M. Laudato, V. Milo, A. Pirovano, P. Fantini, and D. Ielmini, "Unsupervised learning by spike timing dependent plasticity in phase change memory (PCM) synapses," *Front. Neurosci.*, vol. 10, p. 56, 2016.

[8] S. Ambrogio, S. Balatti, V. Milo, R. Carboni, Z.-Q. Wang, A. Calderoni, N. Ramaswamy, and D. Ielmini, "Neuromorphic learning and recognition with one-transistor-one-resistor synapses and bistable metal oxide RRAM," *IEEE Trans. Electron Devices*, vol. 63, no. 4, pp. 1508–1515, 2016.

[9] V. Milo, G. Pedretti, R. Carboni, A. Calderoni, N. Ramaswamy, S. Ambrogio, and D. Ielmini, "Demonstration of hybrid CMOS/RRAM neural networks with spike time/rate-dependent plasticity," *IEDM Tech. Dig.*, pp. 440–443, 2016.

[10] E. Covi, S. Brivio, A. Serb, T. Prodromakis, M. Fanciulli, and S. Spiga, "Analog memristive synapse in spiking networks implementing unsupervised learning," *Front. Neurosci.*, vol. 10, p. 482, 2016.

[11] A. Serb, J. Bill, A. Khiat, R. Berdan, R. Legenstein, and T. Prodromakis, "Unsupervised learning in probabilistic neural networks with multi-state metal-oxide memristive synapses," *Nat. Commun.*, vol. 7, p. 12611, 2016.

[12] G. Pedretti, V. Milo, S. Ambrogio, R. Carboni, S. Bianchi, A. Calderoni, N. Ramaswamy, A. S. Spinelli, and D. Ielmini, "Memristive neural network for on-line learning and tracking with brain-inspired spike timing dependent plasticity," *Sci. Rep.*, vol. 7, p. 5288, 2017.

[13] E. Chicca, F. Stefanini, C. Bartolozzi, and G. Indiveri, "Neuromorphic electronic circuits for building autonomous cognitive systems," *Proc. IEEE*, vol. 102, no. 9, pp. 1367–1388, 2014.

[14] D. Kuzum, R. G. D. Jeyasingh, S. Yu, and H.-S. P. Wong, "Low-energy robust neuromorphic computation using synaptic devices," *IEEE Trans. on Electron Devices*, vol. 59, no. 12, pp. 3489–3494, 2012.

[15] D. J. Amit, *Modeling brain function: The world of attractor neural networks*. Cambridge University Press, 1992.

[16] E. Chicca, D. Badoni, V. Dante, M. D'Andreagiovanni, G. Salina, L. Carota, S. Fusi, and P. Del Giudice, "A VLSI recurrent network of integrate-and-fire neurons connected by plastic synapses with long-term memory," *IEEE Trans. Neural Networks*, vol. 14, no. 5, pp. 1297–1307, 2003.

[17] E. Neftci, J. Binas, U. Rutishauser, E. Chicca, G. Indiveri, and R. J. Douglas, "Synthesizing cognition in neuromorphic electronic systems," *Proc. Natl. Acad. Sci. USA*, vol. 110, no. 37, pp. E3468–E3476, 2013.

[18] N. Qiao, H. Mostafa, F. Corradi, M. Osswald, F. Stefanini, D. Sumislawska, and G. Indiveri, "A reconfigurable on-line learning spiking neuromorphic processor comprising 256 neurons and 128K synapses," *Front. Neurosci.*, vol. 9, p. 141, 2015.

[19] M. Giulioni, F. Corradi, V. Dante, and P. Del Giudice, "Real time unsupervised learning of visual stimuli in neuromorphic VLSI systems," *Sci. Rep.*, vol. 5, p. 14730, 2015.

[20] S. G. Hu, Y. Liu, Z. Liu, T. P. Chen, J. J. Wang, Q. Yu, L. J. Deng, Y. Yin, and S. Hosaka, "Associative memory realized by a reconfigurable memristive Hopfield neural network," *Nat. Commun.*, vol. 6, p. 7522, 2015.

[21] X. Guo, F. Merrikh-Bayat, L. Gao, B. D. Hoskins, B. L.-B. F. Alibart, L. Theogarajan, C. Teuscher, and D. B. Strukov, "Modeling and experimental demonstration of a Hopfield network analog-to-digital converter with hybrid CMOS/memristor circuits," *Front. Neurosci.*, vol. 9, p. 488, 2015.

[22] V. Milo, D. Ielmini, and E. Chicca, "Attractor networks and associative memories with STDP learning in RRAM synapses," *IEDM Tech. Dig.*, pp. 11.2.1–11.2.4, 2017.

[23] S. B. Eryilmaz, D. Kuzum, R. Jeyasingh, S. Kim, M. BrightSky, C. Lam, and H.-S. P. Wong, "Brain-like associative learning using a nanoscale non-volatile phase change synaptic device array," *Front. Neurosci.*, vol. 8, p. 205, 2014.

[24] J. J. Hopfield, "Neural networks and physical systems with emergent collective computational abilities," *Proc. Natl. Acad. Sci. USA*, vol. 79, pp. 2554–2558, 1982.

[25] S. Ambrogio, S. Balatti, D. C. Gilmer, and D. Ielmini, "Analytical modeling of oxide-based bipolar resistive memories and complementary resistive switches," *IEEE Trans. Electron Devices*, vol. 61, no. 7, pp. 2378–2386, 2014.

978-1-5386-4881-0/18/$31.00 ©2018 IEEE